Artificial Intelligence for the Interventional Cardiologist: Powering and Enabling OCT Image Interpretation

Nitin Chandramohan [ID],[1] Jonathan Hinton [ID],[2] Peter O'Kane [ID][2,3] and Thomas W Johnson [ID][1]

1. Translational Health Sciences, University of Bristol, Bristol, UK; 2. University Hospitals Dorset NHS Foundation Trust, Poole, UK; 3. Dorset Heart Centre, Royal Bournemouth Hospital, Bournemouth, UK

Abstract

Intravascular optical coherence tomography (IVOCT) is a form of intra-coronary imaging that uses near-infrared light to generate high-resolution, cross-sectional, and 3D volumetric images of the vessel. Given its high spatial resolution, IVOCT is well-placed to characterise coronary plaques and aid with decision-making during percutaneous coronary intervention. IVOCT requires significant interpretation skills, which themselves require extensive education and training for effective utilisation, and this would appear to be the biggest barrier to its widespread adoption. Various artificial intelligence-based tools have been utilised in the most contemporary clinical IVOCT systems to facilitate better human interaction, interpretation and decision-making. The purpose of this article is to review the existing and future technological developments in IVOCT and demonstrate how they could aid the operator.

Disclosure: TWJ and POK have received consultancy and speaker fees from Abbott Vascular, Boston Scientific and Terumo. TWJ has received research grants from Abbott Vascular. POK is Editor-in-chief of *Interventional Cardiology*; this did not affect peer review. All other authors have no conflicts of interest to declare.
Data availability: Data openly available in a public repository that issues datasets with DOIs.
Correspondence: Thomas W Johnson, University of Bristol, Translational Health Sciences, Level 7, Queen's Building, Bristol Royal Infirmary, Bristol BS2 8HW, UK.
E: tom.johnson@bristol.ac.uk

It is now well established that intracoronary imaging (ICI) in percutaneous coronary intervention (PCI) can improve clinical outcome measures compared with angiography-guided procedures.[1,2] Intravascular optical coherence tomography (IVOCT) is a form of ICI that uses near-infrared light to generate high-resolution, cross-sectional, and 3D volumetric images of the vessel. The short wavelength (1.3 μm) of the infrared light used in IVOCT confers superior axial resolution compared with other ICI modalities, such as intravascular ultrasound (IVUS), making it particularly useful for near-field plaque characterisation.[3,4]

At present, IVOCT is not routinely used in clinical practice, and data from the national audit of percutaneous coronary intervention (NAPCI) highlight that even in high-risk populations, such as in the case of left main PCI, ICI is used only in 66% of left main cases.[5] There is the perception that it prolongs the procedure and that the individual operators' experience with angiography alone is sufficient. Furthermore, there is an additional financial and contrast burden that comes with IVOCT use. Finally, IVOCT requires significant interpretation skills, which themselves require extensive education and training for effective usage, and this would appear to be the biggest barrier to widespread IVOCT adoption.[6]

Artificial intelligence (AI), defined as the theory and development of computer systems able to perform tasks that usually require human intelligence, has the potential to address some of these challenges.

Machine learning (ML) is an application of AI that can function without specific programming and make decisions based on past data.[7] In the context of image interpretation, ML requires the input of expert opinions to discriminate certain features in the image to solve a specific problem. Deep learning (DL) negates the need for feature selection because it automatically extracts essential features from raw input data. Convolutional neural networks are a type of DL algorithm that is well-suited for segmentation, object detection, registration and processing tasks. This then provides the ability to analyse complex images, videos and unstructured data in ways that ML cannot.[7] ML tools have already been used in the most contemporary clinical IVOCT systems to facilitate better human interaction, interpretation and decision-making. This article reviews existing and future technological developments in IVOCT and demonstrates how they can improve IVOCT workflow for the interventional cardiologist.

Co-registration

IVOCT provides detailed assessment of the coronary arteries; however, correlating these findings with the fluoroscopic image can be challenging, for example, translating the optimal stent landing zone from IVOCT to angiography. Angiographic co-registration (ACR) is a process of integrating IVOCT data on an angiographic road map, thereby empowering the operator to effectively use the information. ACR constructs a longitudinal section of the entire vessel length, and the cross-sections of interest can

Figure 1: Example of Ultreon OCT-guided PCI to Mid-left Anterior Descending Artery
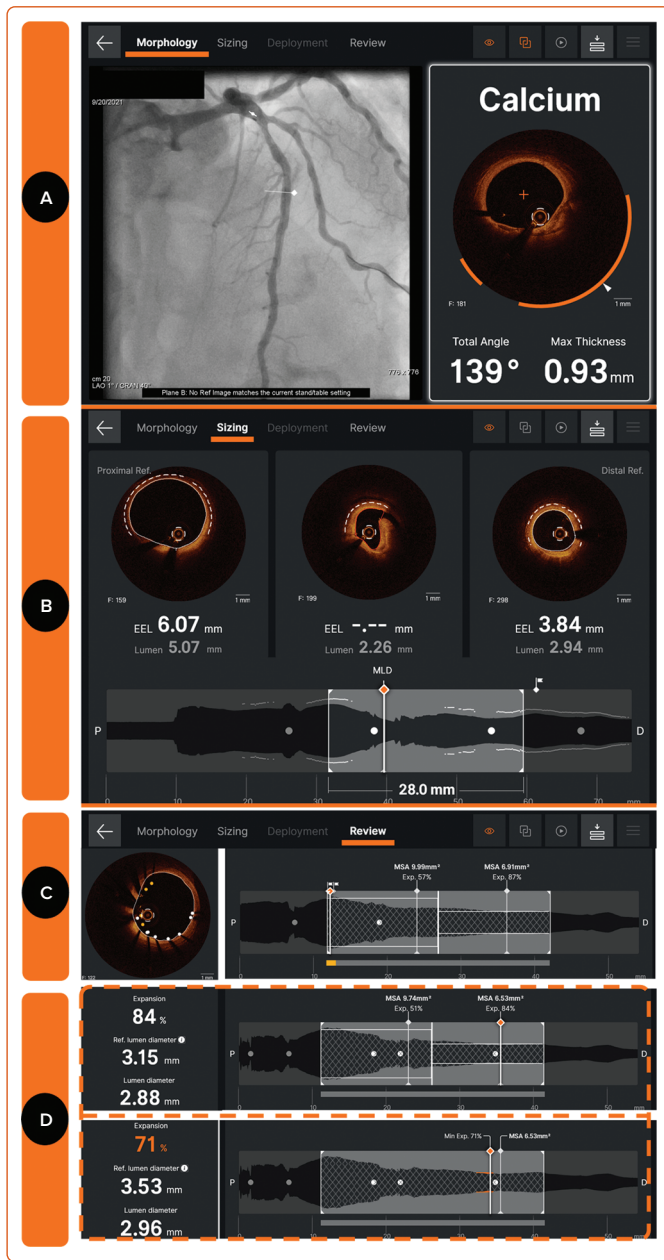
A: Morphological assessment with automated calcium detection, measuring arc, thickness and longitudinal extent of calcium. B: Stent sizing with automated detection of external elastic membrane (EEL; expanded in Figure 2). C: Review of post-stent deployment with automated detection of proximal stent edge malapposition (yellow dots indicate struts >300 μm malapposed and longitudinal extent represented on longitudinal reconstruction). C,D: Automated stent expansion indices can be displayed using ILUMIEN stent half/half (dual) mode (C) and longitudinal reconstruction (D, upper) or tapered mode (D, lower). Dual mode presents proximal and distal segment minimum stent area (MSA) and relative stent expansion according to proximal and distal reference measurements, respectively. Tapered mode achieves a frame-by-frame assessment of expansion, highlighting underexpansion <80% in orange and highlighting the MSA across the entire stented segment. OCT = optical coherence tomography; P = proximal; PCI = percutaneous coronary intervention.

be scrolled through (*Figures 1 and 2*).[8] Where this could be particularly useful is in the treatment of complex bifurcation, or diffuse disease in which spatial orientation is challenging and may require multiple fluoroscopic runs and subsequent excess ionising radiation exposure.[9] A recent study (OPTICO II trial) has shown that ACR significantly improved PCI outcomes by minimising longitudinal geographical mismatch (LGM) and edge dissections compared with IVOCT use with no co-registration.[10]

Figure 2: External Elastic Lamina Detection to Facilitate Stent Sizing
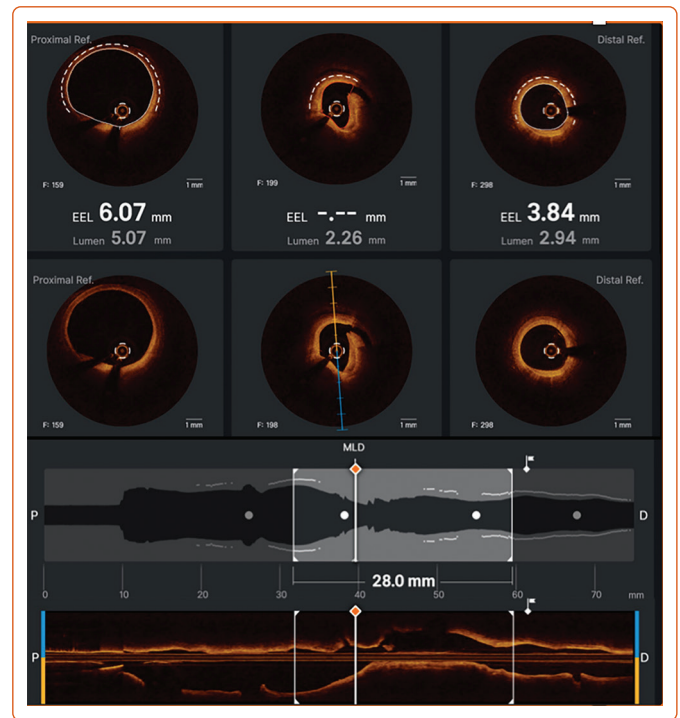
Ultreon-guided vessel sizing for stent selection. Upper panels show automated external elastic lamina (EEL) detection (dashed white line) and lumen contour (solid white line) with averaged EEL and lumen diameters (EEL 6.07 mm proximal and 3.84 mm distal), suggesting a 3.5 mm stent selection (rounding down to the nearest stent size from the smaller distal EEL). Longitudinal reconstruction (lower panels) indicates regions with EEL >180°, suggestive of reasonable landing zones, facilitating a stent selection of 28 mm.

Vessel Dimension Support

Angiography-guided PCI to determine coronary artery vessel diameter and lesion length takes years of experience and is subject to significant error. Enhanced IVOCT software exists that creates a cross-sectional image of the vessel, which incorporates multiplanar reconstruction of the 3D data. Currently, available OCT software (Aptivue/Ultreon, Abbott Vascular [*Figures 1 and 2*] and Lunawave, Terumo) provides automated measurements of the lumen area and diameter. The majority of studies have demonstrated that a larger stent expansion is generally associated with better stent outcomes.[8,11–13]

The use of sizing based on the external elastic lamina (EEL; *Figure 3*) was shown to be a safe approach in the ILUMIEN III study and resulted in comparable stent areas to that of IVUS-guided PCI.[14] ILUMIEN III also identified a significant disparity in the identification of EEL between the trial sites and the IVOCT core lab (*Figure 4*), which subsequently led to the incorporation of automated EEL detection in Ultreon.

Detection of both the EEL and lumen enables assessment of plaque burden, a metric of optimisation used in the ULTIMATE study.[13] Scrolling through the OCT cross-sections enables the operator to determine the proximal and distal landing zones, defined as the segment with minimal atherosclerotic plaque burden and where there is greatest visibility of the EEL (*Figure 2*). The software then automatically calculates the length of the lesion. This approach is said to minimise complications such as LGM, stent edge dissection and, consequently, stent thrombosis further down the line.[15,16] However, when treating diffuse or high-burden disease, a luminal measurement may be preferred to minimise the risk of stent edge mechanical problems.

Figure 3: Bristol Coronary Biobank Co-registered OCT and Trichrome
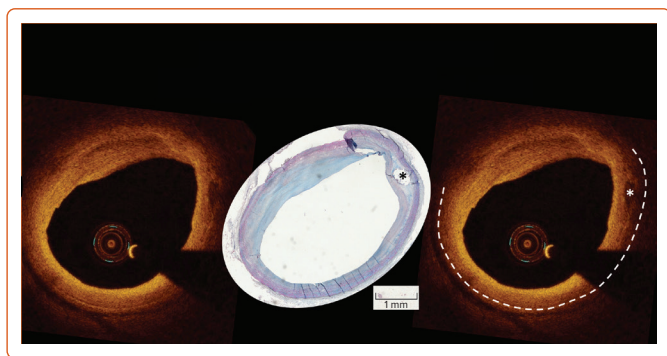
Matched optical coherence tomography (OCT) and trichrome histological specimen highlighting external elastic lamina and media (stained red) and identified on OCT by the dashed white line (the asterisk denotes a small calcified nodule).

Romagnoli et al., who compared various OCT optimisation criteria on the CLIO-PCI 2 cohort, showed that the presence of focal untreated edge disease had a high incidence of device-oriented cardiovascular events with an HR of 8.17.[11] The recently published ILUMIEN IV study, the largest randomised trial comparing IVOCT with angiography, failed to demonstrate a benefit in terms of clinical outcomes at 2 years.[17] On further examination, 9.5% of patients in the IVOCT arm had untreated focal reference segment disease.[17] Furthermore, the in-segment (5 mm upstream and downstream of the stent) minimum luminal diameter was similar at 2.43 mm between the OCT and the angiography arm. This implies that the stents were being deployed in either small calibre vessels or heavily diseased sections of the artery. What this potentially highlights is poor operator–machine interaction and that there is a need for development of automated software that identifies landing zones based on disease burden.

Morphology Assessment

Near-infrared light has distinct backscattering and attenuating characteristics, dependent upon the properties of the tissue being penetrated, with sharp boundaries achieved between distinct vascular tissue layers facilitating high-resolution assessment of the vessel using IVOCT (*Figure 2*). Based on its components, atherosclerotic plaques can be classified as being stable or vulnerable. Stable plaques are characterised by heavy calcification, fibrotic tissue and small lipid pools. Conversely, vulnerable plaques tend to have a large lipid pool (necrotic core) and thin fibrous cap (thin-cap fibroatheroma; TCFA) that is soft in nature and prone to rupture.[4]

In a recent study by Reynolds et al., IVOCT was shown to identify plaque characteristics (plaque rupture, intraplaque cavity and layered plaque) suggestive of a culprit lesion in 46% of the participants with MI associated with non-obstructive coronary arteries (MINOCA).[61] Furthermore, a study by Prati et al. showed that the presence of high-risk plaque characteristics (minimum luminal area <3.5 mm[2], fibrous cap <75 μm, lipid arc >180°, and macrophage infiltration) predicted cardiac death and target lesion MI with an HR of 7.54 (95% CI [3.1–18.6]).[15]

The Combine OCT-FFR trial showed that in patients with diabetes, the presence of TCFA was associated with a fivefold risk of major adverse cardiac events (MACE) despite the absence of ischaemia.[18] Furthermore, the PACMAN-AMI study provided the rationale for identification of vulnerable plaque by demonstrating a reduction in plaque area volume by use of proprotein convertase subtilisin kexin type 9 (PCSK9) inhibitors in such patients.[19] Based on these findings, it is plausible that early

Figure 4: Accuracy in Identifying External Elastic Lamina
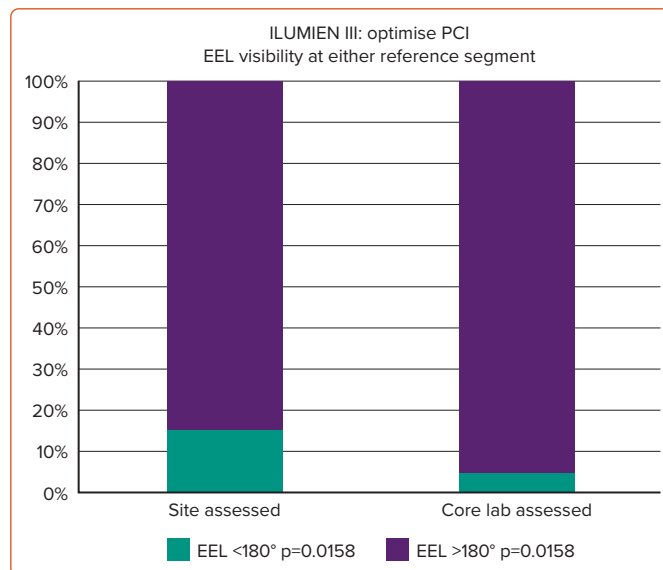
Comparison of site- and core lab-assessed external elastic lamina (EEL) measurements demonstrating a significant inaccuracy of clinical assessment.[14] PCI = percutaneous coronary intervention. Data source: Ali et al. 2016.[14]

identification and treatment of high-risk plaque components with IVOCT could prevent adverse events in the future.

The accurate assessment of lesion morphology will considerably assist the lesion preparation strategy. At one extreme direct stenting may be appropriate in lipid-rich or even largely fibrous plaques to avoid distal embolisation and slow coronary flow. In contrast, some lesions with these characteristics may be deferred for optimal medical therapy to minimise risk of peri-procedural MI. Increasingly, the target lesion contains a moderate to high calcific burden, which may require tools beyond simple balloon dilatation for adequate modification.[20] Recently, an OCT-based calcium scoring tool developed by Fujino et al. showed that a maximum calcium deposit angle >180°, thickness of >0.5 mm, and length >5 mm are predictors of stent underexpansion.[21] Lesions were found to have all three attributes associated with suboptimal stent expansion <70% in 29.2% of the validation cohort. Therefore, in such cases, a more aggressive calcium modification strategy is mandated prior to stenting.[21] The latest IVOCT software (Ultreon) can help accurately delineate calcific arcs and the thickness of the calcium deposit throughout the entire length of the target vessel (*Figures 1 and 5*).[22] However, it is important to note that the accuracy of calcium assessment relies upon adequate blood clearance using contrast media (*Figure 5*).

A few studies have used the DL features of AI to fully automate plaque characterisation using IVOCT, the most recent and noteworthy by Chu et al.[23–25] Chu et al. developed an AI-based tool using a convolutional neural network that comprehensively delineates various plaque constituents in stable patients. The DL algorithm was trained over a large and diverse dataset of IVOCT images, annotated by experienced analysts in order to outline lumen contours, internal elastic lamina, non-tissue parts (stent, wire), plaque components, and markers of inflammation. The dataset consisted of various anatomical morphologies to provide qualitative and quantitative assessment of plaque and vessel components. Initial internal evaluation of the dataset using this AI model showed excellent detection of fibrous, lipid and calcific plaques, with a diagnostic accuracy of 97.6%, 90.5% and 88.5%, respectively. When the model was tested on external

Figure 5: Ultreon Calcium Detection
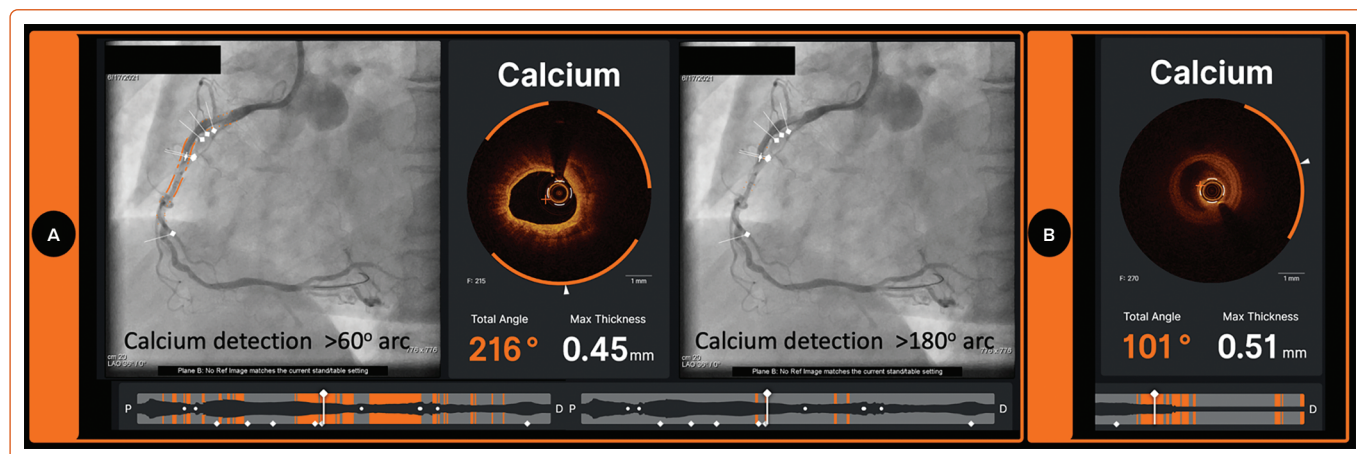
A: Co-registered angiographic and optical coherence tomography (OCT) imaging with calcium highlighted in orange. The left panel shows the presence of calcium with arc > 60° and highlights significant burden extending >5 mm longitudinally. The right panel is configured to demonstrate calcium arc >180° and despite highlighting segments with significant arc (the central OCT frame shows a thin (<0.5 mm) arc of 216°), the longitudinal extent is limited. B: Inaccurate calcium detection generated by poor clearance of blood from the lumen. D = distal; P = proximal.

IVOCT runs, consensus on coronary tissue characterisation could be reached in most of the plaque regions by experts from three OCT core labs. Both the machine algorithm and humans found interpretation of high-attenuating plaque most challenging. Remarkably, the inter-observer agreement for high-attenuating plaques (lipid-rich and macrophagic) was as high as 81.8%. However, the average analysis speed for the AI model was 0.07 ± 0.01 seconds per cross-section, while it took several minutes to annotate one frame in the core lab. Furthermore, image interpretation by AI is enhanced by evaluating multiple IVOCT frames at once. Overall, this AI model has shown the potential to reduce subjectivity in image interpretation and facilitate IVOCT quantification of plaque composition. Further research is needed to assess this model's ability to evaluate patients who present with high-risk lesions.

TCFA and plaque rupture have been strongly associated with acute coronary syndrome.[4] Lee et al. developed an AI model that can automatically detect lipids and assess fibrous cap thickness on IVOCT. This model was able to accurately discriminate lipidic plaques (sensitivity of 85.8%) and clearly identify the fibrous caps in these lesions with minimal inter-observer variance. Albeit optimistic findings, there was a high frequency of false positives attributed to mixed morphology plaques and side branches.[26] Nevertheless, this method holds promise for further research.

Destination Therapy and Concept of MLD MAX
For an AI tool to work, it must rely on expert insights and be trained with the diverse demographic pool that makes up the local population. MLD MAX is an acronym for a prescriptive IVOCT workflow that uses a pre-PCI run to assess morphology, length and diameter (MLD) and a post-PCI run to identify medial dissection, apposition and expansion (MAX). Use of this algorithm in IVOCT represents true systematic implementation of AI. The Lightlab (LL) initiative was specifically designed to assess the impact of this IVOCT workflow on PCI efficiency. The LL programme showed that the implementation of the MLD MAX workflow in IVOCT, when compared with angiography guidance, resulted in lesser radiation exposure, time spent on vessel preparation, and reduction in unplanned treatment at the expense of only 9 additional minutes, on average.[27] These data show that this standardisation of the IVOCT workflow during PCI could possibly improve outcomes without significantly increasing procedure time, and this may result in increased adoption during routine PCI.

Stent Expansion
Stent underexpansion has been consistently demonstrated to be associated with worse longer-term outcomes from PCI.[28–32] As such, the European consensus statement in 2018 recommended stent expansion of greater than 80% of the reference lumen diameter and a minimum stent area of more than 4.5 mm^2 using OCT.[33] The current OCT software provides an automated assessment of the degree of stent expansion (*Figure 1*). Optimal stent expansion could be determined using dual reference areas or through tapered minimum stent expansion. In dual reference mode, expansion is calculated by comparing the respective halves of the stent with either the proximal or the distal reference area. Proximal and distal reference areas are defined as the lumen areas of the first frame outside of the stented segment. In contrast, tapered mode calculates expansion from an interpolated vessel size based on side branches detected by IVOCT (*Figure 1*).[34] The development of AI to guide stent expansion assessment increases the ease of use of the OCT system, which is likely to encourage the use of OCT and, as a result, improve outcomes for patients undergoing PCI. However, how operators interact with theses data is critical for patient outcome. For example, the potential harm of vessel perforation as a result of higher pressure stent post-dilatation should be weighed against a small incremental gain in stent expansion. It is also worth bearing in mind that expansion metrics are reliant upon the selection of proximal and distal reference sites. There will be inaccuracies in the relative expansion if the stent is landed in an area of high disease burden.

Post-procedural assessment with ICI is crucial because it helps evaluate the stent for underexpansion, malapposition, tissue protrusion, edge dissection or LGM (*Figure 1*). In bifurcation PCI, there is evidence to suggest that stent malapposition is a more common finding at the proximal main vessel (MV), and dissection or tissue prolapse in the distal MV.[35]

Specific Areas Where AI Can Add Further Knowledge
Bifurcation
Bifurcation lesions are challenging to manage and tend to be associated with higher rates of adverse cardiac events than non-bifurcation lesions.[36] Procedural planning of bifurcation lesions with only conventional angiography can lead to inaccuracies.[36] IVOCT offers the benefit of being able to clearly illustrate ostial lesions without having to deal with issues

such as overlap and foreshortening.[36] When assessing complex bifurcation lesions with IVOCT, a standalone IVOCT pullback may be required to precisely measure the side branch ostium. However, crossing an IVOCT catheter through the MV stent strut into the side branch carries a risk of stent deformation and other safety concerns. Nonetheless, it has been shown that measurements of the side branch ostium made on cut-plane analysis of the MV OCT pullback are comparable to those from a dedicated side branch IVOCT pullback.[37] Software has now been developed that enables 3D IVOCT reconstruction of coronary bifurcation lesions.[31] For example, the software from Abbott Vascular has a mode wherein the carina and side branch ostia are automatically identified. Not only does this facilitate analysis of the vessel dimensions but also decision-making on the bifurcation stenting strategy.

During a provisional approach bifurcation PCI, a proximal recross will result in an extended metallic neo-carina, and the risk of this is minimised if the distal cell of the jailed side branch ostium is selectively rewired.[38] The position of recrossing of the wire after MV PCI also depends on the stent design and the presence or absence of a strut link in front of the ostium.[39,40] Currently, IVOCT software (Lunawave, Aptivue and Ultreon) has the ability to display the recrossing point in 3D through 'stent enhancement', and enable real-time co-registration with the reconstructed IVOCT image.[41] Imaging-guided recross will not only minimise carinal and side branch struts but it also has the potential to optimise the vessel geometry. Small prospective registries have demonstrated the feasibility of assessment of the guidewire recrossing point after MV stenting using 3D IVOCTs.[39,42,43]

Image acquisition in left main (LM) lesions can be challenging, especially in the case of ostial lesions, in which it is difficult to completely eliminate red blood cells from the aortic root. In contrast, a pilot study assessing the feasibility of IVOCT in LM PCI demonstrated a procedural success (defined as residual angiographic stenosis <50%, TIMI 3 flow in all branches and adequate OCT stent expansion) of 86% in the 70 recruited patients. The 1-year survival free from MACE was 98.6%.[44] Additionally, studies of IVOCT in non-ostial LM lesions have shown that more than 80% of the frames could be analysed and that the majority of the non-analysable frames were from proximal lesions.[45,46] Moreover, the recently published randomised controlled OCTOBER study demonstrated that OCT guidance in LM and non-LM bifurcation PCI had a lower incidence of the primary composite endpoint (MACE) at 2 years compared with angiography only (10.1% versus 14.1%, respectively), and this is despite 15% IVUS use in the angiography arm.[12] The positive results of this study could partly be attributed to the use of a robust OCT workflow for bifurcation PCI. Furthermore, the currently available AI and 3D reconstruction software should drive an increased uptake of IVOCT for bifurcation PCI.

Stent Failure
From IVOCT registries, malapposition, neoatherosclerosis, underexpansion and distal edge dissection have been identified as the major causes of stent thrombosis.[47–49] Regardless of the extent of expansion, stent malapposition has been linked with worse outcomes in the short and long term.[50] Positive vascular remodelling, a consequence of late malapposition, has been linked with late stent thrombosis.[51,52] IVOCT facilitates better identification of neoatherosclerosis and uncovered stent struts, compared with other ICI modalities.[48,53]

Another OCT registry had identified tissue protrusion (extrusion of either tissue or atherothrombotic material from inside the stent) as a predictor of stent thrombosis and is also associated with adverse short-term

outcomes.[54] Irregular protrusion, which confers negative cardiovascular outcomes, is more commonly associated with acute coronary syndrome than stable coronary disease.[55]

IVOCT with ACR could be valuable in the assessment and management of stent failure. Poor vessel expansion and trauma are some of the major factors that contribute to acute and subacute stent thrombosis.[56] In long stented segments, localisation of the stent pathology could facilitate treatment of the precise anatomical location, especially when poorly visualised on angiography. Overall, the co-registration process facilitates easy decision-making without obstructing the workflow of the catheter laboratory.

Automated plaque characterisation through a DL model as described by Chu et al. could be of potential benefit in decision-making when dealing with neoatherosclerosis.[23] According to the current European guidelines, there is a Class I indication for either drug-coated balloon (DCB) or drug-eluting stent (DES) in the treatment of in-stent restenosis. Xhepa et al., in a study of 197 patients, assessed the impact of neointimal pattern seen on IVOCT and treatment modality relative to the outcome.[57] Based on neointimal quadrants, patients were categorised into low or high inhomogeneity groups. Interestingly, DES showed a significant advantage over DCB in the high inhomogeneity group (MACE: HR 0.26, p=0.004; target lesion failure: HR 0.28, p=0.006). However, at this stage, further prospective studies are required to confirm this effect prior to change of standard practice.

Further Research
One of the factors that contributes to poor prognosis in PCI is contrast-induced nephropathy (CIN). The use of dextran or normal saline instead of contrast during IVOCT assessment has been shown to minimise the risk of CIN while producing similar quality images.[8] However, there remain problems with blood mixing, and the potential to provoke arrhythmias with non-contrast flushes.[4] To add to this, the development of an automated IVOCT algorithm based on poor-quality images can be challenging. Non-contrast flushes with similar biocompatibility need to be investigated to minimise these issues.[8]

In current clinical practice there remains a dichotomy between physiology and imaging guidance in PCI. Recently, Yu et al. developed a new approach for rapid computation of virtual fractional flow reserve pullbacks from IVOCT images.[58] Using this technology, an optical flow reserve (OFR) was developed and validated against fractional flow reserve (FFR) to determine the functional significance of coronary artery stenosis. The overall vessel-level diagnostic accuracy of OFR was 90% with a sensitivity of 87% and specificity of 94%, compared with an FFR of ≤0.80 to define physiological significance. These findings seem promising and there is the potential for this technology to be adopted into practice in the near future.

Challenges in Automated IVOCT
Undoubtedly, AI can potentially provide guidance to the interventional cardiologist at each stage of PCI. However, just like the clinician that AI is assisting, there are important limitations that are worth considering. One of the main factors that affects the AI interpretation of vessel size or morphology is the quality of the IVOCT image. The presence of blood swirl due to inadequate clearance or signal dropout due to stent strut or wire will restrict the ability of any AI model to detect tissue characteristics accurately.[8] With the Ultreon software, a poor-quality OCT run can potentially result in both under- and overestimation of calcium, which can

lead to deleterious outcomes when not cross-checked by the operator. In a similar setting, there also remains a possibility that Ultreon can falsely detect EEL, which could lead to inappropriate sizing of devices, thereby leading to unwanted downstream effects.

Current IVOCT software can identify motion artefacts and signal noise in real time. However, it does not have the capability to distinguish between poor-quality pullbacks and other issues such as catheter instability or suboptimal vessel visualisation. A previously proposed segmentation algorithm to detect the quality of pullbacks by Bologna et al. had a modest sensitivity of 76%.[59] Development of AI that can reliably distinguish between inadequate image quality and different tissue morphologies would provide additional benefit to the interventional cardiologist by instructing them that repeat image acquisition was necessary. However, one should always be aware of the possibility that AI algorithms can misidentify structures in the presence of artefacts, especially when the software provides results that seem unusual or inconsistent with clinical judgement. In such cases it is essential to manually review and verify the findings and retain the need for human interaction with AI algorithms.

Before automated IVOCTs can adopted in clinical practice, there are a few aspects that will need to be addressed. First, there is a need for an AI algorithm to be built using a large-scale, expertly annotated dataset. This would then enable the AI model to train and test techniques on data representative of real-world scenarios. Second, to overcome the regulations surrounding updates on medical technology, there needs to be more robust and reliable evidence to justify the use of AI algorithms in routine practice. Finally, issues around data ownership of existing large datasets could limit the rate at which automated software develops.[60] The ability of Ultreon software to self-learn will be limited for this reason, given that companies will need to seek approval prior to adapting any change.

Conclusion

The advent of AI in OCT has improved the ease with which interventional cardiologists use it. Recent data from randomised studies support routine use of ICI to guide PCI. There is now a need for development of software with an improved user interface. Continued growth in this field will result in a greater uptake through improved interpretation, minimising inter-observer variance and significantly reducing procedural time. ❑

1. Gao XF, Ge Z, Kong XQ, et al. 3-year outcomes of the ULTIMATE trial comparing intravascular ultrasound versus angiography-guided drug-eluting stent implantation. *JACC Cardiovasc Interv* 2021;14:247–57. https://doi.org/10.1016/j.jcin.2020.10.001; PMID: 33541535.
2. Hong SJ, Mintz GS, Ahn CM, et al. Effect of intravascular ultrasound-guided drug-eluting stent implantation: 5-year follow-up of the IVUS-XPL randomized trial. *JACC Cardiovasc Interv* 2020;13:62–71. https://doi.org/10.1016/j.jcin.2019.09.033; PMID: 31918944.
3. Ali ZA, Karimi Galougahi K, Maehara A, et al. Intracoronary optical coherence tomography 2018: current status and future directions. *JACC Cardiovasc Interv* 2017;10:2473–87. https://doi.org/10.1016/j.jcin.2017.09.042; PMID: 29268880.
4. Mohan NC, Johnson TW. Intracoronary optical coherence tomography: an introduction. *Catheter Cardiovasc Interv* 2022;(Suppl 1):S57–65. https://doi.org/10.1002/ccd.30583.
5. National Cardiac Audit Programme. *National audit of percutaneous coronary intervention* (*NAPCI*). London: Healthcare Quality Improvement Partnership, 2022. https://www.nicor.org.uk/wp-content/uploads/2022/06/NAPCI-Domain-Report_2022-FINAL.pdf (accessed 1 November 2023).
6. Johnson TW, O'Kane PD. Can machine learned algorithms further illuminate intracoronary imaging in PCI and improve the human touch? *EuroIntervention* 2021;17:18–9. https://doi.org/10.4244/EIJV17I1A3. PMID: 33998525.
7. Gupta R, Srivastava D, Sahu M, et al. Artificial intelligence to deep learning: machine intelligence approach for drug discovery. *Mol Divers* 2021;25:1315–60. https://doi.org/10.1007/s11030-021-10217-3; PMID: 33844136.
8. Ali ZA, Karimi Galougahi K, Mintz GS, et al. Intracoronary optical coherence tomography: state of the art and future directions. *EuroIntervention* 2021;17:e105–23. https://doi.org/10.4244/EIJ-D-21-00089; PMID: 34110288.
9. Mintz GS, Painter JA, Pichard AD, et al. Atherosclerosis in angiographically "normal" coronary artery reference segments: an intravascular ultrasound study with clinical correlations. *J Am Coll Cardiol* 1995;25:1479–85. https://doi.org/10.1016/0735-1097(95)00088-l; PMID: 7759694.
10. Leistner DM, Riedel M, Steinbeck L, et al. Real-time optical coherence tomography coregistration with angiography in percutaneous coronary intervention – impact on physician decision-making: the OPTICO-integration study. *Catheter Cardiovasc Interv* 2018;92:30–7. https://doi.org/10.1002/ccd.27313; PMID: 28940997.
11. Romagnoli E, Burzotta F, Vergallo R, et al. Clinical impact of OCT-derived suboptimal stent implantation parameters and definitions. *Eur Heart J Cardiovasc Imaging* 2023;25:48–57. https://doi.org/10.1093/ehjci/jead172; PMID: 37463223.
12. Holm NR, Andreasen LN, Neghabat O, et al. OCT or angiography guidance for PCI in complex bifurcation lesions. *N Engl J Med* 2023;389:1477–87. https://doi.org/10.1056/NEJMoa2307770; PMID: 37634149.
13. Zhang J, Gao X, Kan J, et al. Intravascular ultrasound versus angiography-guided drug-eluting stent implantation: the ULTIMATE trial. *J Am Coll Cardiol* 2018;72:3126–37. https://doi.org/10.1016/j.jacc.2018.09.013; PMID: 30261237.
14. Ali ZA, Maehara A, Généreux P, et al. Optical coherence tomography compared with intravascular ultrasound and with angiography to guide coronary stent implantation (ILUMIEN III: OPTIMIZE PCI): a randomised controlled trial. *Lancet* 2016;388:2618–28. https://doi.org/10.1016/S0140-6736(16)31922-5; PMID: 27806900.
15. Prati F, Romagnoli E, La Manna A, et al. Long-term consequences of optical coherence tomography findings during percutaneous coronary intervention: the Centro per la Lotta contro l'Infarto – Optimization of Percutaneous Coronary Intervention (CLI-OPCI) LATE study. *EuroIntervention* 2018;14:e443–51. https://doi.org/10.4244/EIJ-D-17-01111; PMID: 29633940.
16. Ino Y, Kubo T, Matsuo Y, et al. Optical coherence tomography predictors for edge restenosis after everolimus-eluting stent implantation. *Circ Cardiovasc Interv* 2016;9:e004231. https://doi.org/10.1161/CIRCINTERVENTIONS.116.004231; PMID: 27688261.
17. Ali ZA, Landmesser U, Maehara A, et al. Optical coherence tomography-guided versus angiography-guided PCI. *N Engl J Med* 2023;389:1466–76. https://doi.org/10.1056/NEJMoa2305861; PMID: 37634188.
18. Kedhi E, Berta B, Roleder T, et al. Thin-cap fibroatheroma predicts clinical events in diabetic patients with normal fractional flow reserve: the Combine OCT-FFR trial. *Eur Heart J* 2021;42:4671–9. https://doi.org/10.1093/eurheartj/ehab433; PMID: 34345911.
19. Räber L, Ueki Y, Otsuka T, et al. Effect of alirocumab added to high-intensity statin therapy on coronary atherosclerosis in patients with acute myocardial infarction: the PACMAN-AMI randomized clinical trial. *JAMA* 2022;327:1771–81. https://doi.org/10.1001/jama.2022.5218; PMID: 35368058.
20. Ono M, Kawashima H, Hara H, et al. Advances in IVUS/OCT and future clinical perspective of novel hybrid catheter system in coronary imaging. *Front Cardiovasc Med* 2020;7:119. https://doi.org/10.3389/fcvm.2020.00119; PMID: 32850981.
21. Fujino A, Mintz GS, Matsumura M, et al. A new optical coherence tomography-based calcium scoring system to predict stent underexpansion. *EuroIntervention* 2018;13:e2182–9. https://doi.org/10.4244/EIJ-D-17-00962; PMID: 29400655.
22. Januszek R, Siłka W, Sabatowski K, et al. Procedure-related differences and clinical outcomes in patients treated with percutaneous coronary intervention assisted by optical coherence tomography between new and earlier generation software (Ultreon™ 1.0 software vs. AptiVue™ software). *J Cardiovasc Dev Dis* 2022;9:218. https://doi.org/10.3390/jcdd9070218; PMID: 35877580.
23. Chu M, Jia H, Gutiérrez-Chico JL, et al. Artificial intelligence and optical coherence tomography for the automatic characterisation of human atherosclerotic plaques. *EuroIntervention* 2021;17:41–50. https://doi.org/10.4244/EIJ-D-20-01355; PMID: 33528359.
24. Gessert N, Lutz M, Heyder M, et al. Automatic plaque detection in IVOCT pullbacks using convolutional neural networks. *IEEE Trans Med Imaging* 2019;38:426–34. https://doi.org/10.1109/TMI.2018.2865659; PMID: 30130180.
25. Abdolmanafi A, Duong L, Dahdah N, Cheriet F. Deep feature learning for automatic tissue classification of coronary artery using optical coherence tomography. *Biomed Opt Express* 2017;8:1203–20. https://doi.org/10.1364/BOE.8.001203; PMID: 28271012.
26. Lee J, Pereira GTR, Gharaibeh Y, et al. Automated analysis of fibrous cap in intravascular optical coherence tomography images of coronary arteries. *Sci Rep* 2022;12:21454. https://doi.org/10.1038/s41598-022-24884-1; PMID: 36509806.
27. Rauch J, Johnson M, Maksoud A, et al. A standardized optical coherence tomography workflow improves procedural efficiency and safety during percutaneous coronary intervention: insights from the LightLab initiative. *J Am Coll Cardiol* 2021;78(19 Suppl S):B113. https://doi.org/10.1016/j.jacc.2021.09.1129.
28. Hong SJ, Kim BK, Shin DH, et al. Effect of intravascular ultrasound-guided vs angiography-guided everolimus-eluting stent implantation: the IVUS-XPL randomized clinical trial. *JAMA* 2015;314:2155–63. https://doi.org/10.1001/jama.2015.15454; PMID: 26556051.
29. Song HG, Kang SJ, Ahn JM, et al. Intravascular ultrasound assessment of optimal stent area to prevent in-stent restenosis after zotarolimus-, everolimus-, and sirolimus-eluting stent implantation. *Catheter Cardiovasc Interv* 2014;83:873–8. https://doi.org/10.1002/ccd.24560; PMID: 22815193.
30. Kang SJ, Ahn JM, Song H, et al. Comprehensive intravascular ultrasound assessment of stent area and its impact on restenosis and adverse cardiac events in 403 patients with unprotected left main disease. *Circ Cardiovasc Interv* 2011;4:562–9. https://doi.org/10.1161/CIRCINTERVENTIONS.111.964643; PMID: 22045969.
31. Kang SJ, Mintz GS, Kim WJ, et al. Changes in left main bifurcation geometry after a single-stent crossover technique: an intravascular ultrasound study using direct imaging of both the left anterior descending and the left circumflex coronary arteries before and after intervention. *Circ Cardiovasc Interv* 2011;4:355–61. https://doi.org/10.1161/CIRCINTERVENTIONS.110.961045; PMID: 21712525.
32. Katagiri Y, De Maria GL, Kogame N, et al. Impact of post-procedural minimal stent area on 2-year clinical outcomes in the SYNTAX II trial. *Catheter Cardiovasc Interv* 2019;93:e225–34. https://doi.org/10.1002/ccd.28105; PMID: 30702187.
33. Räber L, Mintz GS, Koskinas KC, et al. Clinical use of intracoronary imaging. Part 1: guidance and optimization of coronary interventions. An expert consensus document of the European Association of Percutaneous Cardiovascular Interventions. *Eur Heart J* 2018;39:3281–300. https://doi.org/10.1093/eurheartj/ehy285; PMID: 29790954.
34. Volleberg R, Mol JQ, van der Heijden D, et al. Optical coherence tomography and coronary revascularization: from indication to procedural optimization. *Trends Cardiovasc Med* 2023;33:92–106. https://doi.org/10.1016/j.tcm.2021.10.009; PMID: 34728349.
35. Burzotta F, Talarico GP, Trani C, et al. Frequency-domain optical coherence tomography findings in patients with bifurcated lesions undergoing provisional stenting. *Eur Heart J Cardiovasc Imaging* 2014;15:547–55. https://doi.org/10.1093/ehjci/jet231; PMID: 24255135.
36. Collet C, Onuma Y, Cavalcante R, et al. Quantitative

angiography methods for bifurcation lesions: a consensus statement update from the European Bifurcation Club. *EuroIntervention* 2017;13:115–23. https://doi.org/10.4244/EIJ-D-16-00932; PMID: 28067200.

37. Karanasos A, Tu S, van Ditzhuijzen NS, et al. A novel method to assess coronary artery bifurcations by OCT: cut-plane analysis for side-branch ostial assessment from a main-vessel pullback. *Eur Heart J Cardiovasc Imaging* 2015;16:177–89. https://doi.org/10.1093/ehjci/jeu176; PMID: 25227268.

38. Lassen JF, Holm NR, Stankovic G, et al. Percutaneous coronary intervention for coronary bifurcation disease: consensus from the first 10 years of the European Bifurcation Club meetings. *EuroIntervention* 2014;10:545–60. https://doi.org/10.4244/EIJV10I5A97; PMID: 25256198.

39. Okamura T, Onuma Y, Yamada J, et al. 3D optical coherence tomography: new insights into the process of optimal rewiring of side branches during bifurcational stenting. *EuroIntervention* 2014;10:907–15. https://doi.org/10.4244/EIJV10I8A157; PMID: 24531393.

40. Fujino Y, Attizzani GF, Tahara S, et al. Difference in vascular response between sirolimus-eluting- and everolimus-eluting stents in ostial left circumflex artery after unprotected left main as observed by optical coherence tomography. *Int J Cardiol* 2017;230:284–92. https://doi.org/10.1016/j.ijcard.2016.12.122; PMID: 28065691.

41. Nishimura T, Okamura T, Fujimura T, et al. Feasibility, reproducibility and characteristics of coronary bifurcation type assessment by three-dimensional optical coherence tomography. *PLoS One* 2022;17:e0263246. https://doi.org/10.1371/journal.pone.0263246; PMID: 35104282.

42. Okamura T, Onuma Y, Garcia-Garcia HM, et al. High-speed intracoronary optical frequency domain imaging: implications for three-dimensional reconstruction and quantitative analysis. *EuroIntervention* 2012;7:1216–26. https://doi.org/10.4244/EIJV7I10A194; PMID: 22334321.

43. Okamura T, Nagoshi R, Fujimura T, et al. Impact of guidewire recrossing point into stent jailed side branch for optimal kissing balloon dilatation: core lab 3D optical coherence tomography analysis. *EuroIntervention* 2018;13:e1785–93. https://doi.org/10.4244/EIJ-D-17-00591; PMID: 29131806.

44. Amabile N, Rangé G, Souteyrand G, et al. Optical coherence tomography to guide percutaneous coronary intervention of the left main coronary artery: the LEMON study. *EuroIntervention* 2021;17:e124–31. https://doi.org/10.4244/EIJ-D-20-01121; PMID: 33226003.

45. Muramatsu T, García-García HM, Onuma Y, et al. Intimal flaps detected by optical frequency domain imaging in the proximal segments of native coronary arteries: an innocent bystander? Insights from the TROFI trial. *Circ J* 2013;77:2327–33. https://doi.org/10.1253/circj.cj-13-0357; PMID: 23979567.

46. Burzotta F, Dato I, Trani C, et al. Frequency domain optical coherence tomography to assess non-ostial left main coronary artery. *EuroIntervention* 2015;10:e1–8. https://doi.org/10.4244/EIJV10I9A179; PMID: 25599698.

47. Räber L, Mintz GS, Koskinas KC, et al. Clinical use of intracoronary imaging. Part 1: guidance and optimization of coronary interventions. An expert consensus document of the European Association of Percutaneous Cardiovascular Interventions. *EuroIntervention* 2018;14:656–77. https://doi.org/10.4244/EIJY18M06_01; PMID: 29939149.

48. Souteyrand G, Amabile N, Mangin L, et al. Mechanisms of stent thrombosis analysed by optical coherence tomography: insights from the national PESTO French registry. *Eur Heart J* 2016;37:1208–16. https://doi.org/10.1093/eurheartj/ehv711; PMID: 26757787.

49. Choi SY, Witzenbichler B, Maehara A, et al. Intravascular ultrasound findings of early stent thrombosis after primary percutaneous intervention in acute myocardial infarction: a Harmonizing Outcomes with Revascularization and Stents in Acute Myocardial Infarction (HORIZONS-AMI) substudy. *Circ Cardiovasc Interv* 2011;4:239–47. https://doi.org/10.1161/CIRCINTERVENTIONS.110.959791; PMID: 21586693.

50. Maehara A, Ben-Yehuda O, Ali Z, et al. Comparison of stent expansion guided by optical coherence tomography versus intravascular ultrasound: the ILUMIEN II study (observational study of optical coherence tomography [OCT] in patients undergoing fractional flow reserve [FFR] and percutaneous coronary intervention). *JACC Cardiovasc Interv* 2015;8:1704–14. https://doi.org/10.1016/j.jcin.2015.07.024; PMID: 26585621.

51. Lee SY, Hong MK. Mechanisms of stent thrombosis: insights from optical coherence tomography. *J Thorac Dis* 2016;8:e460–2. https://doi.org/10.21037/jtd.2016.04.31; PMID: 27294244.

52. Hassan AK, Bergheanu SC, Stijnen T, et al. Late stent malapposition risk is higher after drug-eluting stent compared with bare-metal stent implantation and associates with late stent thrombosis. *Eur Heart J* 2010;31:1172–80. https://doi.org/10.1093/eurheartj/ehn553; PMID: 19158118.

53. Won H, Shin DH, Kim BK, et al. Optical coherence tomography derived cut-off value of uncovered stent struts to predict adverse clinical outcomes after drug-eluting stent implantation. *Int J Cardiovasc Imaging* 2013;29:1255–63.

https://doi.org/10.1007/s10554-013-0223-9; PMID: 23615849.

54. Soeda T, Uemura S, Park SJ, et al. Incidence and clinical significance of poststent optical coherence tomography findings: one-year follow-up study from a multicenter registry. *Circulation* 2015;132:1020–9. https://doi.org/10.1161/CIRCULATIONAHA.114.014704; PMID: 26162917.

55. Meneveau N, Souteyrand G, Motreff P, et al. Optical coherence tomography to optimize results of percutaneous coronary intervention in patients with non-ST-elevation acute coronary syndrome: results of the multicenter, randomized DOCTORS study (Does Optical Coherence Tomography Optimize Results of Stenting). *Circulation* 2016;134:906–17. https://doi.org/10.1161/CIRCULATIONAHA.116.024393; PMID: 27573032.

56. Witzenbichler B, Maehara A, Weisz G, et al. Relationship between intravascular ultrasound guidance and clinical outcomes after drug-eluting stents: the assessment of dual antiplatelet therapy with drug-eluting stents (ADAPT-DES) study. *Circulation* 2014;129:463–70. https://doi.org/10.1161/CIRCULATIONAHA.113.003942; PMID: 24281330.

57. Xhepa E, Bresha J, Joner M, et al. Clinical outcomes by optical characteristics of neointima and treatment modality in patients with coronary in-stent restenosis. *EuroIntervention* 2021;17:e388–95. https://doi.org/10.4244/EIJ-D-20-00662; PMID: 32894230.

58. Yu W, Huang J, Jia D, et al. Diagnostic accuracy of intracoronary optical coherence tomography-derived fractional flow reserve for assessment of coronary stenosis severity. *EuroIntervention* 2019;15:189–97. https://doi.org/10.4244/EIJ-D-19-00182; PMID: 31147309.

59. Bologna M, Migliori S, Montin E, et al. Automatic segmentation of optical coherence tomography pullbacks of coronary arteries treated with bioresorbable vascular scaffolds: application to hemodynamics modeling. *PLoS One* 2019;14:e0213603. https://doi.org/10.1371/journal.pone.0213603; PMID: 30870477.

60. Carpenter HJ, Ghayesh MH, Zander AC, et al. Automated coronary optical coherence tomography feature extraction with application to three-dimensional reconstruction. *Tomography* 2022;8:1307–49. https://doi.org/10.3390/tomography8030108; PMID: 35645394.

61. Reynolds HR, Maehara A, Kwong RY, et al. Coronary optical coherence tomography and cardiac magnetic resonance imaging to determine underlying causes of myocardial infarction with nonobstructive coronary arteries in women. *Circulation* 2021;143:624–40. https://doi.org/10.1161/CIRCULATIONAHA.120.052008; PMID: 33191769.